Journal of Computers Vol. 30 No. 4, 2019, pp. 17-30
doi:10.3966/199115992019083004002

A Modified Direct Search Algorithm Based on Kernel Density Estimator with Three Mapping Strategies for Solving Nonlinear Optimization

Lin-Lin Zhang[1], Bin Mu[1], Shi-Jin Yuan[1*]

[1] School of Software Engineering, Tongji Univeristy, Shanghai, China
{1310787, binmu}@tongji.edu.cn, yuanshijin2003@163.com

Received 22 September 2017; Revised 21 March 2018; Accepted 31 March 2018

Abstract. The direct search algorithm is an effective way to solve constrained nonlinear optimization problems in the fields of physics. In this paper, we propose a modified direct search algorithm based on kernel density estimator (called MDSA for short), and aim to investigate whether it can be applied to solve the constrained nonlinear optimization problems with higher dimensions. To improve the strategy of producing initial values for increasing the convergence rate and resulting precision, we adopt three mapping strategies to guide the initial value, including the logistic map, sine map and tent map. Eight classical test functions are investigated for evaluating the performance of the MDSA. And the initial values also are produced by the random way for comparison on the mean run time, best value, mean value, root mean square error (RMSE), and iterator number of the convergence of the best objective value with those three mapping strategies. The experimental results show that: (1) For all test functions, the results with the mapping strategies are almost better than those with the random way. (2) To the first solution of every test function with the different initial values, the sine map can obtain the most stable solution. (3) The sine map achieves the best value in the four test functions. (4) The tent map outperforms at obtaining the minimum of the objective value of the initial particle. In conclusion, MDSA is an effective method for solving constrained nonlinear optimization problems with higher dimensions, and the sine map is suggested for producing the initial values. In addition, this paper can provide some new ideas for solving constrained nonlinear optimization problems with higher dimensions in the field of physics.

Keywords: direct search algorithm, logistic mapping, sine mapping, tent mapping

1 Introduction

Constrained nonlinear optimization problems are the cores of the study of various physical phenomena. For instance, solving conditional nonlinear optimal perturbation is a typical constrained nonlinear optimization problem and the core of studying the typhoon adaptive observations [1-2], the predictability of El Niño-Southern Oscillation prediction [3-4], and the double-gyre variation [5]. To solve such constrained nonlinear optimization problems, many methods have been proposed, including steepest descent method (SDM) [6], conjugate gradient method [7], quasi-newton method [8], and spectral projected gradient (SPG) [9]. And all the algorithms need the gradient information to guide the optimal direction. But not all problem models can provide the corresponding gradient information, and the development of the corresponding adjoint scheme is a very time-consuming and complicated work. Therefore, it is necessary to develop an efficient search optimize algorithm without using the gradient information, such as the direct search algorithms [10-14].

There are two main advantages for adapting the direct search algorithms. First and foremost, it does not need to use the gradient information for guiding its optimization. In fact, a large number of constrained nonlinear optimization problems are non-differentiable, and it means that there does not exist

* Corresponding Author

the gradient information. Using the methods based on the gradient information cannot obtain the optimum value or fail to optimize. Second, it is easy to implement and works well. Bagde et al. proposed a biogeography- based optimization algorithm combining time domain simulations and direct method to solve transient stability constrained optimal power flow, and the simulation results shown that the proposed algorithm is capable of obtaining higher quality solutions [10]. Porcelli and Toint proposed a direct-search derivative-free optimizer, named Brute Force Optimizer, for solving bound-constrained problems, and obtained the conclusion that it was also applicable to multilevel equilibrium- or constrained-type problems [11]. Pillo et al. developed a DIRECT-type algorithm with a derivative-free local minimization of a nonsmooth exact penalty function for solving bound constrained optimization problems without using derivatives, and the reported numerical results shown the efficiency and robustness of the approach both in terms of feasibility and optimality [12]. Custódio and Madeira proposed a new class of algorithms based on the directional direct search coupled and applied them to solve global derivative-free optimization problems, and the numerical results shown that the proposed method was competitive with currently commonly used global derivative-free optimization solvers [13]. Cheung and Gu proposed a direct search algorithm based on kernel density estimator to solve nonlinear optimization, and found that it was an effective algorithm and had potential due to its structure [14].

The dimensions of researches [10-14] are all not more than 50. But constrained nonlinear optimization problems in the fields of physics always have strong-nonlinearity and high dimensions, at least 10^2 dimensions. The algorithm proposed by Cheung and Gu [14] is more suitable for such constrained nonlinear optimization problems, because it only needs to calculate the objective values of the problem in a local hypercube to obtain the approximate ascent direction from density estimator, which is a scheme based on the distribution feature of the original data samples without using the prior knowledge and can avoid the deviation of the given model and the actual model. However, the authors of the study [14] only adopted two test functions in the numerical experiments, and the dimension of the solution space only upped to 30. It is necessary to investigate whether it can be applied to solve the constrained nonlinear optimization problems with higher dimensions. In addition, their initial values are produced by the random way, but the initial value will affect the convergence rate. Hence, it is needful to improve the strategy of producing initial values.

To increase the convergence rate and resulting precision of the direct search method, using chaotic mapping strategy is an expected choice. He et al. applied the improved logistic map to enhance the effectiveness and robustness of particle swarm optimization (PSO) algorithm [15]. Yuan et al. proposed a paralleled continuous tabu search algorithm to solve conditional nonlinear optimal perturbation, and used the sine map to produce the initial particle. The experimental results shown that the sine map was helpful for rapid convergence rate [16]. Jiang applied the improved tent map combined with the alopex heuristic algorithm to a hybrid optimization algorithm, and the convergence speed and global optimal value of the presented algorithm are thus improved [17].

Combined with the above mentioned, we propose a modified direct search algorithm based on the kernel density estimator (called MDSA for short) with three mapping strategies for solving the constrained nonlinear optimization problems with higher dimensions. The mapping strategies include the logistic map, sine map and tent map. Specifically, MDSA samples a set of trial points centered at a given point and utilizes the kernel density estimator of the neighborhood of this point for estimating the next search direction. To evaluate the performance of the MDSA with the different mapping strategies, we adopt eight classic test functions. For comparing with the original DSA, we also generate the initial value with the random way. The four groups of experiments are compared on the terms of the mean run time, best value, mean value, root mean square error (RMSE), and iterator number of the convergence with the best objective value. After the analysis of these results, we will offer some suggestions on how to choose the mapping strategies in the optimization of constrained nonlinear problems.

Overall, our aims in this paper are:

(i) To investigate whether the DSA can be applied to solve the constrained nonlinear optimization problems with higher dimensions.

(ii) To improve the strategy of producing initial values for increasing the convergence rate and resulting precision.

(iii) To suggest how to choose the mapping strategies in the optimization of constrained nonlinear problems.

Through the experiment and analysis, this paper also can provide some new ideas for solving constrained nonlinear optimization problems with higher dimensions in the field of physics.

The remainder of this paper is organized as follows: Section 2 describes the theory of the direct search algorithm based on kernel density estimator with the three mapping strategies. Section 3 presents the design and analysis of numerical experiments. Summaries and conclusions are denoted in section 4.

2 The Theory of MDSA Method

In this section, we introduce the theory of MDSA method. MDSA has four main steps: the initialization of particles with chaotic maps, the calculation of the objective function, the approximation of the search direction, the verification of the termination condition. The framework of the MDSA method is given in Algorithm 1, and its steps are described in detail in the following subsections.

Algorithm 1. Modified direct search algorithm based on the kernel density estimator (MDSA)

Initialization. Generate n initial particles $\{x_1, x_2, \ldots\ldots, x_n\}$ with the logistic map Eq. (1), sine map Eq. (2) and tent map Eq. (3).

Until convergence or reaches the maximum

(1) Keep the best solution. Calculate the objective values of every particle of the test function in Table 1, and save the largest value and the corresponding particle as the optimal initial particle for input of the MDSA method.

(2) Produce M neighbors in the local hypercube. Produce M neighbors, $\{y_1, y_2, y_3, \ldots, y_M\}$, of the initial particle x^t in a local region, which are distributed in a hypersphere with *h* radius.

(3) Calculate and save the objective values. Calculate and save the objective values of the neighbors using the formulas in Table 1.

(4) Approximate ascent direction from density estimator. Use the kernel function to obtain the density estimation of x^t for updating the particle, the way of updating is displayed in Eq. (4) - Eq. (6).

(5) Estimate the particle. If $f(x^{t+1}) > f(x^t)$, replace x^t with x^{t+1}

Output: the best particle and value.

2.1 The Initialization of Particles with Three Chaotic Maps

To obtain an optimal initial particle, we apply three chaotic mapping strategies to produce the initial particles, and select the best one as the first input of the MDSA method.

Logistic map. The logistic map [18] is a typical mapping of the complex nonlinear behavior, also called as parabolic mapping. Mathematically, the logistic map is written as

$$x_{n+1} = \mu x_t (1 - x_n). \tag{1}$$

where x_n is a number belong to (0, 1), μ is an adjustable parameter in the interval [0, 4]. x_{n+1} is the value of x_n after mapping. When μ is changed, the equation will display the different dynamics extreme behaviors, including the stable points ($0 < \mu < 3$), periods ($3 < \mu < 3.6$), and chaotic system ($\mu > 3.6$).

In this paper, we set $\mu = 4$ for the uniform distribution of the particles to find the optimal initial particle.

Sine map. The sine map [19] is applied to many studies because of its special domain [-1, 1]. Compared to the logistic map, the sine map has larger Lyapunov exponents [20], and the adjustable parameter α has wider range. The mathematical definition of the sine map is as follows:

$$x_{n+1} = \alpha \sin(x_n). \tag{2}$$

where x_n is a real number, and x_{n+1} is the value of x_n after mapping, and α is the adjustable parameter. We set $\alpha = 1$ in this paper.

Tent map. In mathematics, the tent map [21] is a piecewise linear mapping and its shape likes a tent. The real-valued function of the tent map is defined by

$$x_{n+1} = \begin{cases} \varphi x_n & , \quad 0 < x_n < \dfrac{1}{2} \\ \varphi(1-x_n) & , \quad \dfrac{1}{2} < x_n < 1 \end{cases}. \tag{3}$$

where x_n is a number in the range (0, 1), φ is the adjustable parameter in the interval (0, 2). When $\varphi > 1$, the function is in the chaotic system. In this paper, we set $\varphi = 2$.

These three mapping strategies are used to find the optimal initial particle. Therefore, the adjustable parameter of every strategy is set as the value bringing the chaotic system.

2.2 The Approximation of the Search Direction

In this paper, we adopt the kernel density estimator to approximate the search direction of the next iterator [14]. To estimate the value of function $f(x)$ by the kernel density estimator with *S* neighbors $\{y_1, y_2, y_3, \ldots, y_S\}$ in a local hypercube with radius, there is

$$f(x)_S = \frac{V_{D_x}}{Sh^n} \sum_{i=1}^{S} f(y_i) k(\cdot). \tag{4}$$

where V_{D_x} is the volume of the hypercube D_x, whose center is *x*. *n* is the number of dimensions of the constrained nonlinear function $f(x)$. $f(y_i)$ is the objective value of the neighbor y_i of the according function, $i = \{1, 2, \ldots\ldots, S\}$. $k(\cdot)$ is the kernel function, i.e. 2-norm as follows.

$$k(\cdot) = \| \frac{y_i - x}{h} \|^2 . \tag{5}$$

The ascent direction of the kernel density estimator $f(x)_S$ at particle x^t is

$$\Delta p = \frac{\sum_{i=1}^{S} f(y_i) k(\cdot) y_i}{\sum_{i=1}^{S} f(y_i) k(\cdot)} - x^t . \tag{6}$$

Hence, there is

$$x^{t+1} = x^t + \Delta p. \tag{7}$$

In Eq. (7), the superscript *t* represents the number of iterator, Δp is the increment of the particle x^t in the next iterator $t+1$.

2.3 The Calculation of the Objective Value of the Test Function

To verify the effectiveness of the MDSA method, we adopt eight classical test functions to verify the effectiveness of the MDSA method, including four unimodal test functions and multimodal test functions. And all the test functions need to be solved the minimum. Taking the Ackley function as a case, we describe the details of the calculation of the objective value of the test function. The formula of Ackley function is as follows:

$$f(x) = -20e^{-\frac{1}{5}\sqrt{\frac{1}{D}\sum_{i=1}^{D} x_i^2}} - e^{\frac{1}{D}\sum_{i=1}^{D}\cos(2\pi x_i)} + e + 20 \tag{7}$$

The dimension of the Ackley function can be changed, the D in Eq. (7) represents the dimension. When D is set as 2, the spatial distribution of the Ackley function is plotted in Fig. 1.

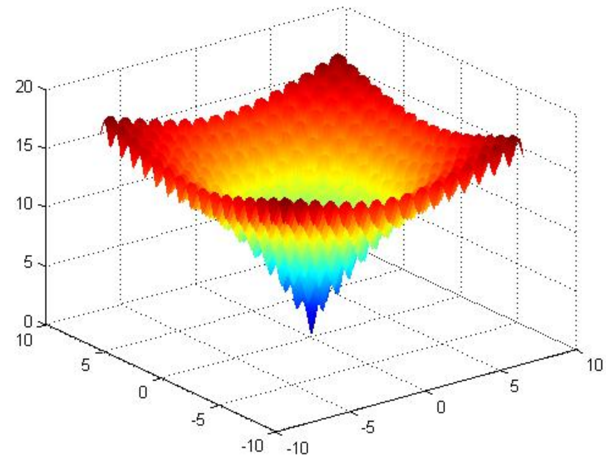

Fig. 1. The spatial distribution of the Ackley function

From the Fig. 1, we can find that this function has many local minimums, the global minimum is 0 in the point (0, 0). Hence, with increasing dimensions, achieving the global minimum is more difficult.

The other seven test function are listed in Table 1.

Table 1. The list of the test function in this paper.

Name	Formula	Global minimum	Type
Quadric	$f(X)=\sum_{i=1}^{D} i x_i^4 + random(0,1)$	$X^*=(1,1,\cdots,1),\ f(X^*)=0$ $Subject\ to\ x_i \in [-30, 30]$	Unimodal
Sphere	$f(X)=\sum_{i=1}^{D} x_i^2$	$X^*=(0,0,\cdots,0),\ f(X^*)=0$ $Subject\ to\ x_i \in [-1.5, 1.5]$	Unimodal
Brown	$f(X)=\sum_{i=1}^{D-1}(x_i^2)^{(x_{i+1}^2+1)}+(x_{i+1}^2)^{(x_i^2+1)}$	$X^*=(0,0,\cdots,0),\ f(X^*)=0$ $Subject\ to\ x_i \in [-1, 4]$	Unimodal
Sum	$f(X)=\sum_{i=1}^{D} i x_i^2$	$X^*=(0,0,\cdots,0),\ f(X^*)=0$ $Subject\ to\ x_i \in [-100, 100]$	Unimodal
Griewank	$f(X)=\frac{1}{4000}\sum_{i=1}^{D} x_i^2-\prod_{i=1}^{D}(\cos(\frac{x_i}{\sqrt{i}}))+1$	$X^*=(0,0,\cdots,0),\ f(X^*)=0$ $Subject\ to\ x_i \in [-600, 600]$	Multimodal
Rastrigin	$f(X)=100D+\sum_{i=1}^{D}(x_i^2-10\cos(2\pi x_i))$	$X^*=(0,0,\cdots,0),\ f(X^*)=0$ $Subject\ to\ x_i \in [-10, 10]$	Multimodal
Ackley	$f(x)=-20e^{-\frac{1}{5}\sqrt{\frac{1}{D}\sum_{i=1}^{D}x_i^2}}-e^{\frac{1}{D}\sum_{i=1}^{D}\cos(2\pi x_i)}+e+20$	$X^*=(0,0,\cdots,0),\ f(X^*)=0$ $Subject\ to\ x_i \in [-32, 32]$	Multimodal
Schaffer	$f(x)=\frac{\sin^2\sqrt{x_1^2-x_2^2}-0.5}{[1+0.001(x_1^2+x_2^2)]}+0.5$	$X^*=(0,0),\ f(X^*)=0$ $Subject\ to\ x_i \in [-100, 100]$	Multimodal

3 Experiments and Analysis

In this section, we design four groups of experiments, and mark them as the ways of producing the initial particle, respectively. We evaluate the results in the terms of the mean run time, best value, mean value, RMSE, and iterator number of the convergence with the best objective value. We also analyze the objective values of the optimal initial particle of every test function. One goal of this study is to investigate the effect of the mapping strategies on the initial particle. Another purpose is to offer some suggestions on how chooses the mapping strategy for solving nonlinear optimization.

All experiments are executed in the personal computer with the intel core i7-6700, and the random-access memory (RAM) is 16.0 GB. The core processor is 64 bits with 3.40GHz. The program is developed by the Eclipse IDE for Java Developers Neon.3 Release (4.6.3).

3.1 The Analysis of the Objective Value of the Initial Particle with the Different Mapping Strategies

In this subsection, we execute the program of the MDSA 20 times with the given setting for every test function. And the initial particle as the input of the MDSA is achieved by the four diverse ways, i.e., the random way, the logistic map, the sine map and the tent map. In total, the program is executed for 640 time. We plot all the objective values of the optimal initial particles in Fig. 2.

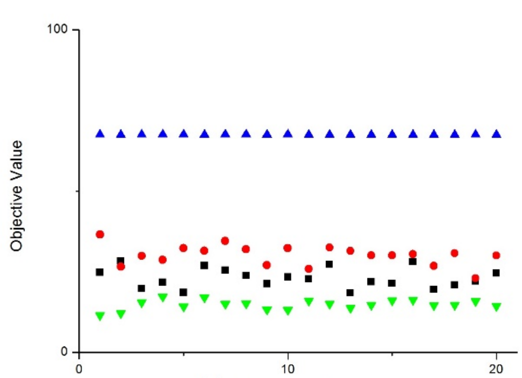

Subfigure (a) is the Sphere function

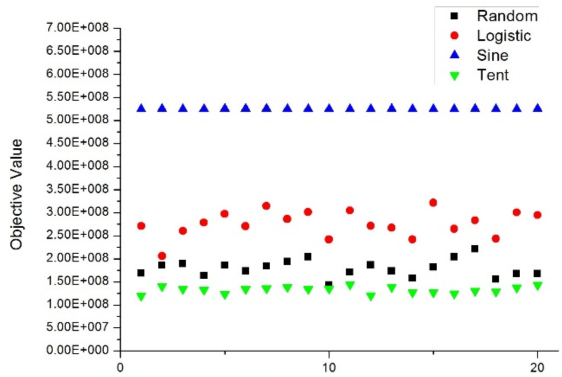

(b) is the Quadric function

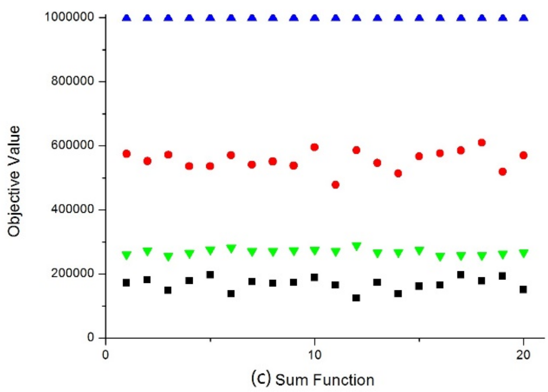

(c) is the Sum function

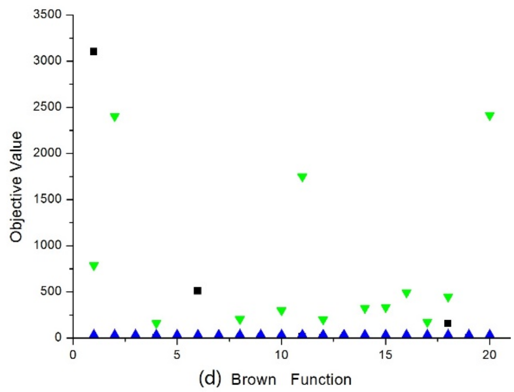

(d) is the Brown function

Fig. 2. The objective values of the initial particles of the test functions with the different mapping strategies. The black squares describe the values of the random way, the logistic mapping is represented as the red circles, the blue up-triangles denote the values of the sine mapping, and the green down-triangles are from the tent mapping

In Fig. 2, the points are all the objective values of the four test functions, and the four colors represent the four ways of producing the initial particles. Subfigure (a) is the results of the Sphere function, (b) is the Quadric function, (c) is the Sum function, and (d) is the Brown function. These four functions are all unimodal functions. In this figure, we can conclude that:

(1) The random way achieves the optimal initial particle with the minimum objective value sometimes.

(2) The sine mapping strategy achieves the most stable performance, because the distributions of the objective values of these four test functions like straight lines almost.

(3) The logistic mapping strategy shows a trend of oscillation in Fig. 2(a) Fig. 2(c).

(4) The tent mapping strategy can obtain the optimal initial particle with the minimum of the objective values for two test functions.

Concretely, in Fig. 2(a), Fig. 2(b) and Fig. 2(c), the four ways of producing the initial particles have the similar distribution. The tent mapping can obtain the initial particle with the minimums of the objective values. And the objective values of the logistic map and random way have the similar shock locations with a little trend of oscillation. The largest objective values are gained from the sine map, but we want to find the minimum. In other words, the tent map achieves the best initial particles in the Sphere, Quadirc and Sum function. The subfigure Fig. 2(d) of Fig. 2 has only the values of the sine map, tent map and random way, because the logistic map produces the initial particles having too large objective values, and the values are out of range of the precision of double real type, we cannot read the values, but this does not influence the following solution. Moreover, the random way has only three points, also because the display of the large values will decrease the readability of the subfigure. But, the randomness of the random way also can be realized. The sine map obtains the minimums for the first time in the Brown function.

The objective values of the Ackley function, Schaffer function, Rastrigin function, and Griewank function are presented in Fig. 3.

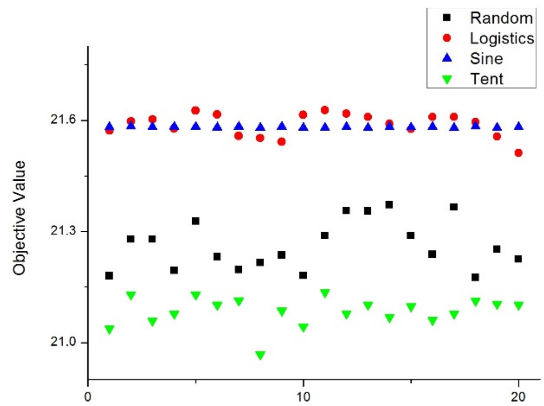

Subfigure (a) is the Ackley function

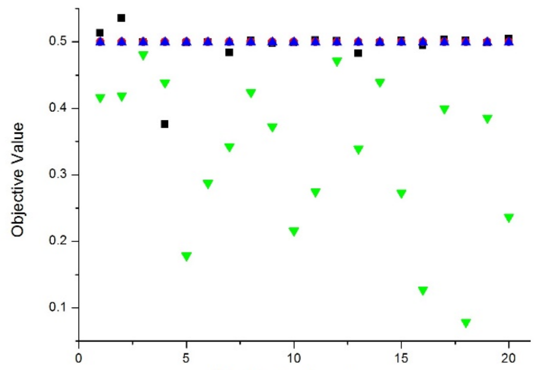

(b) is the Schaffer function

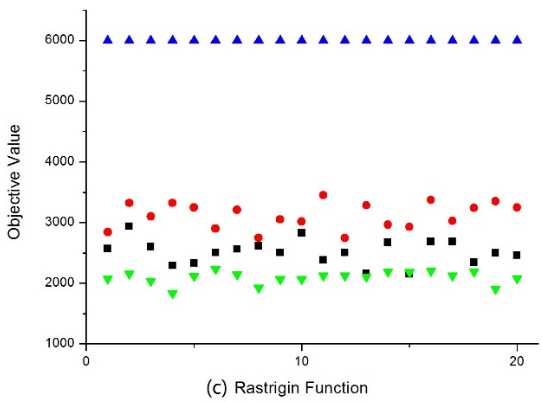

(c) is the Rastrigin function

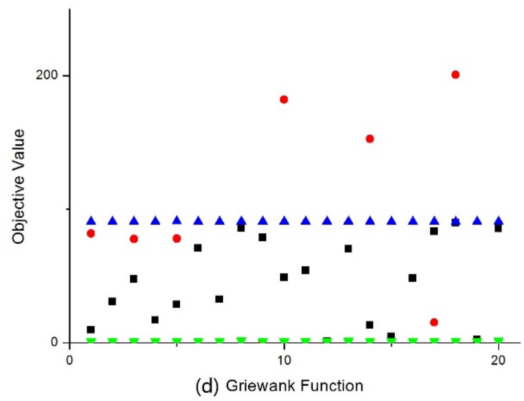

(d) is the Girewank function

Fig. 3. The objective values of the initial particles of the test functions with the different mapping strategies. The black squares describe the values of the random way, the logistic mapping is represented as the red circles, the blue up-triangles denote the values of the sine mapping, and the green down-triangles are from the tent mapping

In Fig. 3, these four test functions are all the multimodal functions. Every subfigure is different from the others, but the sine map also performs the best stability and the tent map obtains the minimum objective values of all the test functions. Especially, the logistic map in the subfigures (a) shows the obvious trend of oscillation with the smooth curve. And the distributions of the objective values from the random ways are scattered, but the values are much closer to the minimums comparing with the logistic map and sine map.

Concretely, the Fig. 3(a) and Fig. 3(c) have the similar distribution diagrams with the Fig. 2(a), Fig.

2(b) and Fig. 2(c). But in the Fig. 3(a), the values of the logistic map are higher than those of the sine map. For the subfigure Fig. 3(b), the values of the logistic map and sine map are almost overlapped, and the tent map obtains the best objective values. For the Fig. 3(d), due to the objective values of the logistic map covers an enormous range, we do not plot them all in the subfigure considering that the lack of the values does not affect the meaning of the figure, and other values should also be presented clearly. The locations of the objective values from the sine map and tent map are plotted like lines, which show the stability of them. The random way generates the random initial particles with the values distributing between those of the sine map and the tent map.

Combined with the Fig. 2 and Fig. 3, we summarize three points:

(1) The sine mapping strategy has the best stability, maybe because its periodic domain.

(2) No matter how distributed the values are, the tent map can obtain the minimum of the objective value of the initial particle, except for the Brown function.

(3) The logistic mapping strategy gains the different optimal initial particle everytime, but the distribution of the objective values of the particles has the trend of oscillation more or less.

3.2 The Analysis of the Details of the Initial Particle with the Different Mapping Strategies

To investigate the details of the initial particles from the four producing ways, we plot them in the Fig. 4 and Fig. 5. As the setting dimensions of the test functions are more than 20 excepting for the Schaffer function, the spatial positions of the particle cannot be displayed in the horizontal coordinate. Hence, we describe them in the horizontal coordinate as a one-dimensional vector. And it is unpractical to show all 20 initial particles in one subfigure, we only plot one particle for one producing way.

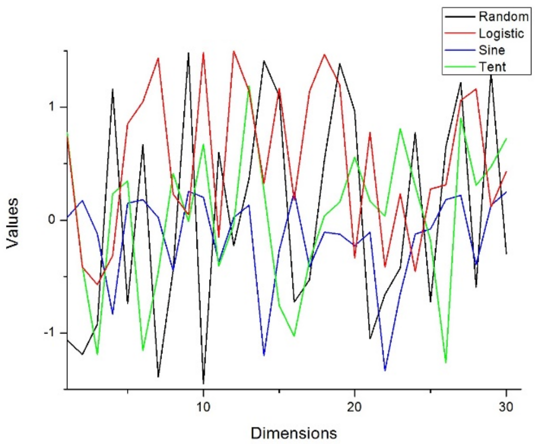

(a) Quadric function

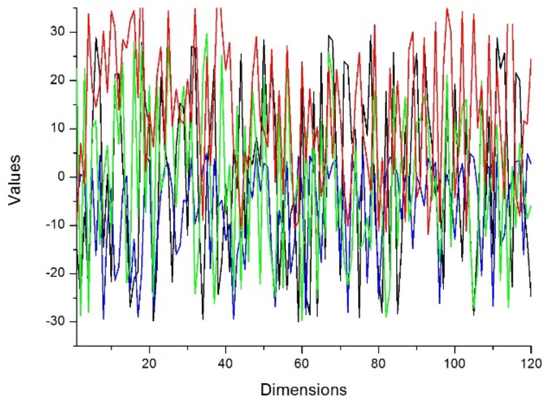

(b) Sum function

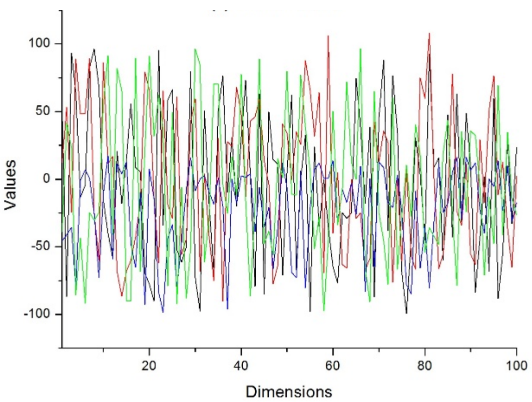

(c) Brown function

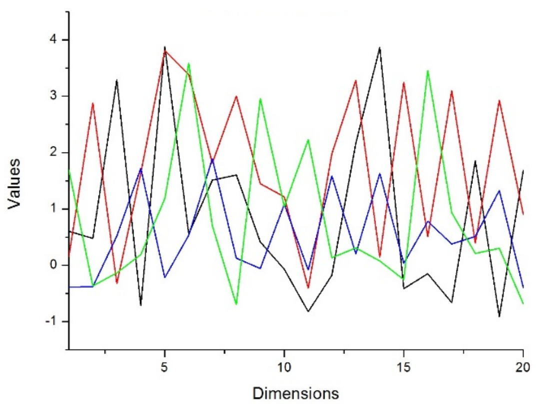

(d) The black line is from the random way, the logistics mapping is represented as the red line, the blue line describes the sine mapping, and the green line denotes the tent mapping

Fig. 4. The value of every dimension of the initial particles for the Sphere function

For the Fig. 4, we can find the distributions of the values of the initial particles are all scattered but with oscillation. And the different mapping strategies have their own fields. In the Fig. 4(a), most of the values of the logistic map are greater than 0, while most of the sine map' values are less than 0. And the values of the tent map and random way are distributed in all the domain of definition, but the values of the tent map are more regular, i.e., one is greater than 0 and the next one is less than 0. The Fig. 4(b) is similar with the Fig. 4(a), but has more obvious fields' distributions. But for subfigures Fig. 4(c) and Fig. 4(d), the sine map keeps the similar distribution with the subfigure Fig. 4(a) and Fig. 4(b), but the logistic map covers the larger region. The tent map also moves regularly. The random way retains its own property, randomness.

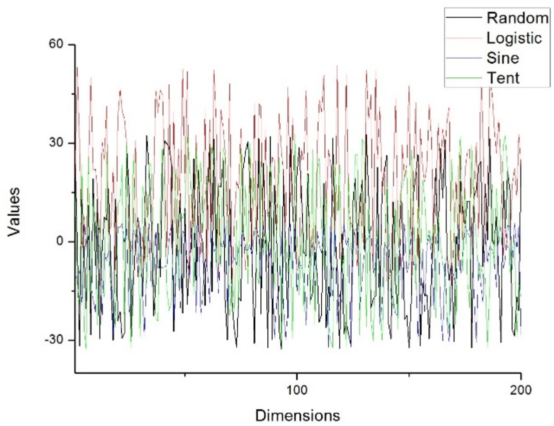

(a) Schaffer function

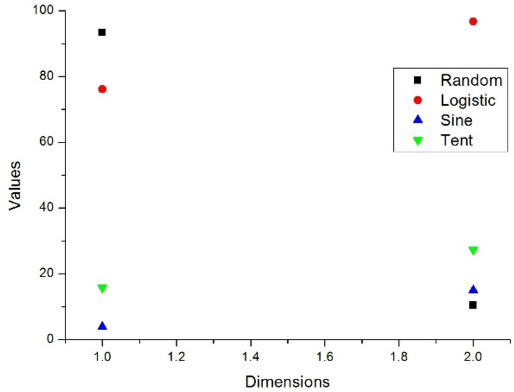

(b) Rastrigin function

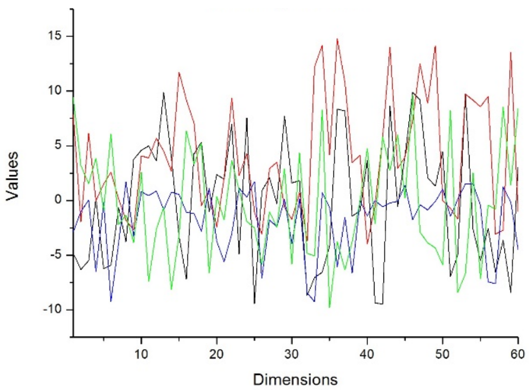

(c) Girewank function

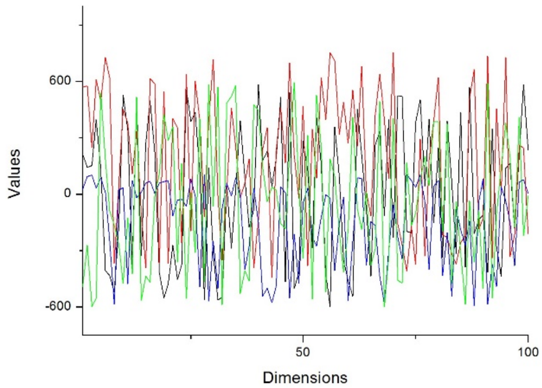

(d) The black line and squares are from the random way, the logistics mapping is represented as the red line and circles, the blue line and up-triangles describe the sine mapping, and the green line and down-triangles denote the tent mapping

Fig. 5. The value of every dimension of the initial particles for the Ackley function

In the Fig. 5, the distributing fields are similar with the Fig. 4. Most values of the logistic map are plotted on the upper half of the whole domain of definition, and the sine map on the lower half domain. And the tent map follows the moving rule, i.e. one goes up and the next goes down. There is a special subfigure, Fig. 5(b), as the Schaffer function has only 2 dimensions, its distributing rule cannot be embodied. But the logistic map also has the larger values in the particles.

Overall, no matter which type the function is, the same mapping strategy has the similar influence on the distribution of the values of the particle, which hinges on its own mathematical formula. But the setting of the adjustable parameter should be payed attention, because it will affect the dispersion of the chaotic system.

In addition, we also find that the values from the sine map are located near to 0, which very likely increases the convergence speed.

3.3 The Analysis in the Terms of Mean Run Time, Best Value, Mean Value and RMSE

In this subsection, we analyze the experiments in the terms of mean run time, best value, mean value, RMSE and iterator number of the convergence with the best objective value. There are two terminal conditions of the MDSA program. One condition is that the maximum of iterator number is 100, and the other condition is the threshold ε. Once the program satisfies one condition of them, it ends. The program is executed 20 times for every test function with the diverse ways of producing the initial particles. And the results are shown in Table 2. For eight test functions, we set different dimensions for investigating their influence on the performance of the MDSA method. The Schaffer function has 2 dimensions. The dimensions of the other seven test functions are set at 20, 30, 60, 100, 100, 120, 200, respectively.

Table 2. The analysis of the experimental results in the terms of mean run time, best value, mean value, RMSE and iterator number of the convergence with the best objective value. In the table E-XX denotes the style of scientific notation, in which the value is represented as a floating-point number multiplied by an integral power of 10

Function	dimensions	Map	Mean run time (ms)	Best value	Mean value	RMSE	Iterator number
Schaffer	2	Random	27.5	4.21E-07	1.24E-02	0.027983819	21
		Logistic	**26.4**	1.08E-06	9.97E-03	0.015540842	32
		Sine	**26.4**	**1.44E-07**	**1.65E-03**	**0.005528414**	**19**
		Tent	27.3	3.02E-07	3.33E-02	0.063814434	43
Brown3	20	Random	188	1.39E-07	1.44E-07	5.00E-09	39
		Logistic	**186**	1.28E-07	1.43E-07	7.85421E-09	70
		Sine	**186**	**1.27E-07**	**1.39E-07**	5.56859E-09	70
		Tent	**186**	1.37E-07	1.45E-07	**4.89117E-09**	**34**
Sphere	30	Random	74.7	4.73E-08	5.16E-08	1.6135E-09	79
		Logistic	75	**4.70E-08**	5.16E-08	2.01784E-09	20
		Sine	**74**	4.71E-08	**5.03E-08**	1.85482E-09	**4**
		Tent	76.2	4.92E-08	5.14E-08	**1.24418E-09**	49
Rastrigin	60	Random	233	4.62E-06	5.16E-06	2.12241E-07	91
		Logistic	**231**	4.82E-06	5.18E-06	1.42286E-07	82
		Sine	232	**4.70E-06**	**5.10E-06**	1.27721E-07	**5**
		Tent	**231**	5.01E-06	5.23E-06	**1.18483E-07**	64
Sum	100	Random	**179**	1.53E-08	1.61E-08	3.65921E-10	6
		Logistic	**179**	1.58E-08	1.61E-08	**3.12288E-10**	38
		Sine	**179**	**1.43E-08**	**1.57E-08**	6.43877E-10	**5**
		Tent	180	1.49E-08	1.60E-08	4.56958E-10	56
Griewank	100	Random	407	2.34E-10	2.59E-10	**1.49295E-11**	**43**
		Logistic	414	2.14E-10	2.58E-10	1.80139E-11	64
		Sine	405	2.08E-10	**2.48E-10**	2.33798E-11	88
		Tent	**403**	**1.96E-10**	2.50E-10	2.37392E-11	75
Quadric	120	Random	419	4.89E-05	5.45E-05	2.86166E-06	51
		Logistic	412	5.04E-05	5.46E-05	2.6851E-06	51
		Sine	**410**	**4.70E-05**	**5.37E-05**	**2.62927E-06**	**41**
		Tent	414	4.92E-05	5.47E-05	3.14438E-06	**41**
Ackley	200	Random	719	**2.49E-05**	2.56E-05	2.50199E-07	**18**
		Logistic	**706**	2.50E-05	2.56E-05	**2.11375E-07**	36
		Sine	710	2.51E-05	2.56E-05	2.99692E-07	28
		Tent	720	2.50E-05	2.56E-05	3.12951E-07	64

Mean run time. The mean run time is the mean value of the run time of the 20 experiments with the four ways of generating the initial particles. The unit is millisecond (ms).

For the Schaffer function, the minimum of the mean run time is 26.4 ms, and the optimal initial particles are obtained from the logistic map and sine map. For the Brown3 function, the three mapping strategies have the same mean run time, 186 ms, which is smaller than the random way's. For the Sphere function, the sine map achieves the minimal mean run time, 74 ms. For the Rastrigin function, the logistic map and tent map get the minimum, 231 ms. For the Sum function, in addition to the tent map, the other three strategies all have the minimum mean run time, 179 ms. For the Griewank function, the minimum of the mean run time is 403 ms from the tent map. For the Quadric function, the minimum time is acquired by the sine map, which is 410 ms. For the Ackley function, the logistic map gains the minimum mean run time 706 ms. In conclusion, except for the Sum function, the mean run time of every test function is decreased by the mapping strategies.

Best value. The best value is the best objective value of the 20 experimental results.

The best values are gained from the sine map in the Schaffer, Brown3, Rastrigin, Ackley, Sum, and Quadric function. For the Sphere function, the logistic map achieves the best value. For the Griewank function, it is the tent map who obtains the best value. Obviously, all the best values of these test functions are obtained from the program with the mapping strategies. This also proves that the mapping strategies are effective in improving the precision of the objective values of the test functions.

Mean value. The mean value is the mean objective value of the 20 experimental results.

The mean value can be used to inspect the mapping strategies affected the stability of the MDSA method. The smaller value is, the more stable means. In addition to the Ackley function, the minimum values of the other seven test functions are all obtained from the sine map. This conclusion proves that the MDSA method with the sine map has the best stability in the three mapping strategies.

RMSE. RMSE is the way of investigating the precision of the solution of the MDSA method with the different mapping strategies. The smaller RMSE is, the higher precision is. And the mathematical definition of RMSE is described in the following formula.

$$RMSE = \sqrt{\frac{\sum_{i=1}^{n}(X_{obs,i} - X_{model,i})^2}{n}} \qquad \textbf{(8)}$$

where $X_{obs,i}$ is the objective value of every experiment of one test function, and $X_{model,i}$ is the best one of all the $X_{obs,i}$ for simulating the true value of the function, *n* is the number of the $X_{obs,i}$, which is 20 in this paper.

In the Quadric and Schaffer function, the sine map has the minimum RMSE, and it means that the MDSA method with this mapping strategy can achieve the highest precision. For the Sphere, Rastrigin and Brown3, the tent map is the best one. And the logistic map outperforms the others in the Ackley and Sum function. Only for the Griewank function, the random way has the best result, but the RMSE of the logistic map is very close to it. These results also mean that the mapping strategies are effective on the increasing the precision of the results.

Iterator number of the convergence with the best objective value. It is the iterator number of the best objective value appearing for the first time, which also means the iterator number of the convergence of the MDSA method.

For the Schaffer function, 19 is the minimum of the iterator number, and from the sine map. For the Brown3 function, the minimum iterator number (34) is obtained from the tent map. For the Sphere, Rastrigin, and Sum function, the sine map achieves the minimal iterator numbers, 4, 5 and 5, respectively. In the Griewank function, the minimum of the iterator number is 43 and from the random way. For the Quadric function, the minimum time is acquired by the sine map and tent map, which is 41. For the Ackley function, it is the random way who gains the minimum iterator number 18.

In this part, the sine map performs well, and it obtains the best objective value fastest in four test functions.

Combined with the above analysis on the five terms, including the mean run time, best value, mean value, RMSE and iterator number of the convergence with the best objective value, we can conclude that the mapping strategies are effective in increasing the convergence speed and the improving the precision of the results. Especially, the sine map performs the best of the three mapping strategies.

4 Summaries and Conclusions

To solve constrained nonlinear optimization problems with high dimensions, direct search method is an expected choice, because it has two main preponderance. One is that direct search method is free of gradient information. In fact, many constrained nonlinear optimization problems of various fields are nondifferentiable, and that means the gradient information is inexistent. The other one is the simple implements of direct search methods. But this type methods have some limitations, such as slowly converge and inapplicable for the high-dimensional solution space.

Based on the study [14], first we investigate whether the algorithm can be applied to solve the constrained nonlinear optimization problems with higher dimensions. To increase the convergence rate and resulting precision, we adopt the chaotic maps as the strategies of producing initial values. Then, according the numerical experiments and analysis, we will suggest how to choose the mapping strategies in the optimization of constrained nonlinear problems.

Therefore, in this paper, we propose a modified direct search algorithm based on kernel density estimator (called MDSA for short) for solving nonlinear optimization problems. We adopt three mapping strategies to produce the initial particle, including the logistic map, sine map and tent map. To evaluate the effectiveness of the MDSA, we use eight classical test functions as the objective functions to solve their minimums. For comparison of the mean run time, best value, mean value, root mean square error (RMSE), and iterator number of the convergence of the best objective value with the above three mapping strategies, the initial particles also are produced by the random way.

In addition to the analysis of the above five terms, we first investigate the objective values of the test functions with the four ways of producing the initial particles. The distribution rule of every producing way is also investigated by plotting the values of every dimension of the initial particle. We conclude four points as follows:

(1) The sine mapping strategy has the best stability, maybe because its periodic domain.

(2) No matter how distributed the values are, the tent map can obtain the minimum of the objective value of the initial particle, except for the Brown function.

(3) The logistic mapping strategy gains the different optimal initial particle everytime, but the distribution of the objective values of the particles has the trend of oscillation more or less.

(4) Most values from the logistic map are plotted on the upper half of the whole domain of definition, and the sine map on the lower half domain. And the tent map follows the moving rule, i.e. one goes up and the next goes down.

To analyze the experimental results on the mean run time, best value, mean value, RMSE, and iterator number of the convergence of the best objective value with the above three mapping strategies, we have five conclusions:

(1) Except for the Sum function, the mean run time of every test function is decreased by the mapping strategies.

(2) All the best values of these test functions are obtained from the program with the mapping strategies.

(3) The MDSA method with the sine map has the best stability in the three mapping strategies.

(4) The mapping strategies are effective on the increasing the precision of the results.

(5) The sine map performs well, and it obtains the best objective value fastest in four test functions.

All experiments and analysis illustrate that the MDSA with the different mapping strategy is an effective method for solving constrained nonlinear optimization problems with higher dimensions. And all conclusions prove that the mapping strategies are effective in increasing the convergence speed and improving the precision of the results. Especially, the sine map performs the best of the three mapping strategies. Hence, the sine map is our final suggestion.

Currently, the MDSA is only applied to solve the minimums of the test functions, and the number of dimensions is 200. The runtime of serial MDSA is acceptable for now. Our further work is applying it to solve constrained nonlinear optimization of actual physical problem, for instance, solving conditional nonlinear optimal perturbation to identify the sensitive areas of tropical cyclone adaptive observations, which is a brand-new attempt for this field. And the dimension of solving conditional nonlinear optimal perturbation is about 105-107. To solve this problem, we need to revamp or redo the codes of the MDSA for applying to the new problem and parallel it to accelerate the solving procedure.

Acknowledgements

In this paper, the research was sponsored by the Foundation of National Natural Science Fund of China (No. 41405097).

References

[1] Y. Li, S. Peng, D. Liu, Adaptive observation in the South China Sea using CNOP approach based on a 3-D ocean circulation model and its adjoint model, Journal of Geophysical Research Oceans 119(12)(2014) 8973-8986.

[2] L.-L. Zhang, S.-J. Yuan, B. Mu, F.-F. Zhou, CNOP-based sensitive areas identification for tropical cyclone adaptive observations with PCAGA method, Asia-Pacific Journal of Atmospheric Sciences 53(1)(2017) 63-73.

[3] R.-H. Zhang, L.-J. Tao, C. Gao, An improved simulation of the 2015 El Niño event by optimally correcting the initial conditions and model parameters in an intermediate coupled model, Climate Dynamics 6(2017) 1-14.

[4] B. Mu, L.-L. Zhang, S.-J. Yuan, H.-Y. Li, PCAGA: Principal component analysis based genetic algorithm for solving conditional nonlinear optimal perturbation, in: Proc. International Joint Conference on Neural Networks IEEE, 2015.

[5] S.-J. Yuan, M. Li, B. Mu, J.-P. Wang, PCAFP for Solving CNOP in Double-Gyre Variation and Its Parallelization on Clusters, in: Proc. International Conference on High PERFORMANCE Computing and Communications, International Conference on Smart City, International Conference on Data Science and Systems, 2016.

[6] P. Debye, Näherungsformeln für die Zylinderfunktionen für große Werte des Arguments und unbeschränkt veränderliche Werte des Index, Mathematische Annalen 67(4)(1909) 535-558.

[7] M.R. Hestenes, E. Stiefel, Methods of conjugate gradients for solving linear systems, Journal of Research of the National Bureau of Standards 49(6)(1952) 409-436.

[8] M.H. Loke, R.D. Barker, Rapid least-squares inversion of apparent resistivity pseudosections by a quasi-Newton method, Geophysical Prospecting 44(1)(1996) 131-152.

[9] E.G. Birgin, J.M. Martínez, M. Raydan, Spectral projected gradient methods: review and perspectives, Journal of Statistical Software 60(3)(2013) 1-21.

[10] B.Y. Bagde, B.S. Umre, K.R. Dhenuvakonda, An efficient transient stability-constrained optimal power flow using biogeography-based algorithm, International Transactions on Electrical Energy Systems 28(1)(2018) e2467.

[11] M. Porcelli, P.L. BFO Toint, A Trainable Derivative-free Brute Force Optimizer for Nonlinear Bound-constrained Optimization and Equilibrium Computations with Continuous and Discrete Variables, ACM, 2017.

[12] G. Di Pillo, G. Liuzzi, S. Lucidi, S. Lucidi, F. Rinaldi, A DIRECT-type approach for derivative-free constrained global optimization, Computational Optimization & Applications 65(2)(2016) 361-397.

[13] A.L. Custódio, J.F.A. Madeira, GLODS: global and local optimization using direct search, Journal of Global Optimization 62(1)(2015) 1-28.

[14] Y.-M. Cheung, F. Gu, A direct search algorithm based on kernel density estimator for nonlinear optimization, in: Proc. International Conference on Natural Computation, 2014.

[15] Y. He, S. Yang, Q. Xu, Short-term cascaded hydroelectric system scheduling based on chaotic particle swarm optimization using improved logistic map, Communications in Nonlinear Science & Numerical Simulation 18(7)(2013) 1746-1756.

[16] S. Yuan, Y. Qian, B. Mu, Paralleled continuous Tabu search algorithm with sine maps and staged strategy for solving CNOP, in: Proc. Algorithms and Architectures for Parallel Processing, 2015.

[17] S.-H. Jiang, Chaotic hybrid optimization algorithm of a new Skew Tent map, Control Theory & Applications 24(2)(2007) 269-273.

[18] R.M. May, Simple mathematical models with very complicated dynamics, Nature 261(5560)(1976) 459-467.

[19] C.C. Lalescu, Patterns in the sine map bifurcation diagram, International Surgery 100(6)(2012) 1104-1110.

[20] A, Wolf, J.B. Swift, H.L. Swinney, J.A. Vastano, Determining Lyapunov exponents from a time series, Physica D: Nonlinear Phenomena 16(3)(1985) 285-317.

[21] D. Lai, G. Chen, M. Hasler, Distribution of the lyapunov exponent of the chaotic skew Tent map, International Journal of Bifurcation & Chaos 09(10)(1999) 2059-2067.